International Journal of Thin Films Science and Technology

http://dx.doi.org/10.18576/ijtfst/140207

An In-Depth Analysis of Investigating and Simulating Thin Film Materials Using the Sputtering Process in Plasma Environments

*KOULALI Mostefa and BOUAZZA Abdelkader**

L2GEGI Laboratory, University of Tiaret, 14000 Tiaret, Algeria

Received: 11 Jan. 2025, Revised: 13 Mar. 2025, Accepted: 15 Mar. 2025.
Published online: 1 May 2025.

Abstract: Sputtering takes place when ions strike a surface, leading to the ejection of atoms from that material. The yield of sputtering is affected by factors like the energy of the incoming ions and their angle of impact. In our initial study, we aim to quantify the sputtering yield of copper (Cu), silicon (Si), and indium oxide (In_2O_3) when bombarded by argon (Ar) and xenon (Xe) ions using SRIM software. We start by calculating the yield for normal incidence before exploring various angles of approach. The findings are then compared to analytical models, such as the Yamamura and Tawara model, to validate the SRIM results. This comparison confirms SRIM's effectiveness in predicting sputtering yield across different plasma conditions, establishing its dependability for future simulations of sputtering processes.

Keywords: SRIM, Monte Carlo simulations, angular distribution, sputtering yield, energy distribution, sputtering process

1 Introduction

A layer or series of layers with thicknesses ranging from nanometers (often called monolayers) to several micrometers is referred to as a thin film. Stacking multiple thin films creates a multilayer structure, which is often applied to a substrate for various purposes, including protection, aesthetic enhancement, and modification of optical or electrical properties [1-3].

Significant importance is placed on thin film deposition, a process that involves applying a thin layer of material onto a surface, which may be a substrate or previously deposited layers. Techniques for deposition can be broadly categorized into two groups based on their predominant physical or chemical characteristics. This thesis will concentrate on the most widely used techniques within this domain.

Numerous everyday applications rely on thin films, such as mirrors, which are made from glass coated with thin layers of metals like aluminum or silver. These reflective surfaces are produced using deposition methods such as spray coating or sputtering. The 20th century saw technological advancements in thin film deposition techniques, leading to breakthroughs in various fields, including optical coatings, electronic semiconductor devices, hard coatings for cutting tools, magnetic recording media, integrated passive devices, LEDs, and energy solutions like thin film solar cells and batteries [4-7].

Among the primary methods for developing thin films are Physical Vapor Deposition (PVD) and Chemical Vapor Deposition (CVD). While physical deposition methods are typically used in research settings, chemical methods are favored in industrial applications due to their higher yields, superior film quality, and capability for selective deposition. In our research, sputtering deposition will be utilized as a technique for creating thin films [8,9].

Theoretical calculations of sputtering yield will be performed using the Yamamura and Tawara theory, with SRIM software chosen for simulating the bombardment of noble gases (Ar and Xe) on three

widely used materials in technology: copper (Cu), indium oxide (In_2O_3), and silicon (Si). This study aims to investigate the influence of various parameters, such as energy and angle of incidence, on thin film growth.

2 Components Incorporated in the Model

Copper is highly valued for its ease of processing and exceptional thermal and electrical conductivity, making it a crucial material in various industries. While historically abundant, recent closures of copper mines have raised

*Corresponding author E-mail: Abdelkader.bouazza@univ-tiaret.dz

© 2025 NSP
Natural Sciences Publishing Cor.

significant concerns regarding the future availability of this essential metal. This situation coincides with an increased demand for copper in critical sectors, such as renewable energy, lithium batterie and next-generation power transmission infrastructure. The surge in the use of copper foil in lithium batteries has further intensified demand, leading to higher prices for copper and prompting innovative strategies to optimize the utilization of thin copper films. These developments reflect the ongoing importance of copper in advancing technological applications and highlight the need for sustainable management of this valuable resource [10].

Silicon serves a fundamental role in semiconductor technology, primarily due to its outstanding electronic properties, high charge carrier mobility, and well-established fabrication techniques that facilitate its widespread use. The significance of silicon became particularly evident in the 1970s, especially in the realm of thin film solar cells. Unlike traditional silicon wafer cells, thin-film solar cells made from silicon offer notable advantages, including reduced material requirements and enhanced material efficiency, which contribute to lower production costs. Additionally, silicon's unique characteristics mean that it does not necessitate exceptionally high absorption efficiency compared to alternative semiconductor materials. This allows researchers to focus their efforts on optimizing other critical aspects of cell design and the manufacturing processes involved, ensuring that silicon remains a dominant material in solar energy applications [11].

Indium tin oxide (ITO) thin films have garnered extensive research interest due to their significant role in the field of optoelectronic. ITO films are recognized as n-type semiconductors that exhibit a resistivity ranging from 10^-3 to 10^-4 ohm-cm, making them suitable for a variety of applications. These films are widely used in photovoltaic cells, transistors, transparent conductive electrodes in solar cells, liquid crystal displays, gas sensor devices, and organic light-emitting diodes (OLEDs). A range of synthesis methods has been employed to produce ITO films, including R.F. magnetron sputtering, thermal evaporation, and chemical vapor deposition, each offering unique advantages for different applications. Current research continues to focus on enhancing the performance and broadening the functionality of ITO thin films, ensuring their ogoing relevance and adaptability in a diverse array of technological applications [12].

3 Applying the Yamamura and Tawara Model to Sputtering Yield Assessment

The Yamamura-Tawara model is a well-established tool in the fields of materials science and engineering, widely utilized for simulating and analyzing cathodic sputtering processes. This empirical fitting formula, referred to as Y(E), proves particularly effective for materials composed of multiple components. Its significance lies in its ability to provide accurate predictions of sputtering yields across different conditions, making it invaluable for both theoretical studies and practical applications. By accounting for various factors, such as ion energy and incident angle, the model allows researchers to optimize sputtering processes and develop advanced materials. Consequently, the Yamamura-Tawara model has become a fundamental resource for understanding the complexities of sputtering in various technological contexts [13-20].

$$Y(E) = 0{,}042 \times \frac{Q(Z_2)a\left(\frac{M_1}{M_2}\right)}{U_S} \times \frac{S_n(E)}{1+\mathrm{G}Kee^{0{,}3}} \times \left(1-\sqrt{\frac{E_{\mathrm{tht}}}{E}}\right)^{s} \quad (1)$$

- ✓ $\boldsymbol{\varepsilon}$: The reduced energy
- ✓ α :is an energy independent function of the ration of ions and target masses
- ✓ $\boldsymbol{Sn}$: The nuclear stopping power of the target
- ✓ $\boldsymbol{Us}$: the surface binding energy
- ✓ Γ : parameter that factor in the contribution of reflected ions to the recoil cascade and takes the form:

$$\mathrm{G} = \frac{W(Z_2)}{1+\left(\frac{M_1}{7}\right)^3} \quad (2)$$

And we have:

$$W = 0{,}35 \times Us \quad (3)$$

Where Z1 and M1 are the atomic number and mass of the probe ion (here argon) and Z2 and M2 are those for the target atoms. Eth is the threshold energy.

$$E_{th} = \begin{cases} \left(1+5{,}7\times\frac{M_1}{M_2}\right)\times\frac{U_s}{?} & \text{when } M_1 < M_2 \\ 6{,}7\times\left(\frac{U_s}{\gamma}\right) & \text{when } M_1 > M_2 \end{cases} \quad (4)$$

With the elastic collisions is:

$$\gamma = \frac{4\times M_1\times M_2}{(M_1+M_2)^2} \quad (5)$$

Here we use the nuclear stopping power of the target given by:

$$S_n(E) = 84{,}78\frac{Z_1\times Z_2}{\left(Z_1^{\frac{2}{3}}+Z_2^{\frac{2}{3}}\right)^{\frac{1}{2}}} \times \frac{M_1}{M_1+M_2} \times S_n(e) \quad (6)$$

Where Z_1 and Z_2 are the atomic number and mass of the probe ion and M_1 and M_2 are similarly for the target atoms where the inelastic electronic stopping power is:

$$S_n(\varepsilon) = \frac{3{,}441\times\sqrt{\varepsilon}\times\ln(\varepsilon+2{,}718)}{1+6{,}355\times\sqrt{\varepsilon}+\varepsilon\left(6{,}882\times\sqrt{\varepsilon}-1{,}708\right)} \quad (7)$$

© 2025 NSP
Natural Sciences Publishing Cor.

And if E is in eV we have:

$$\varepsilon = \frac{0{,}03255}{Z_1 \times Z_2 \left(Z_1{}^{2/3} + Z_2{}^{2/3}\right)^{1/2}} \times \frac{M_2}{M_1 + M_2} \times E \quad (8)$$

The expression of α When $M_1 \geq M_2$

$$\alpha = 0{,}088 \times \left(\frac{M_2}{M_1}\right)^{-0{,}15} + 0{,}165 \times \left(\frac{M_2}{M_1}\right) \quad (9)$$

When $M_1 \leq M_2$:

$$\alpha = 0{,}249 \times \left(\frac{M_2}{M_1}\right)^{0{,}56} + 0{,}0035 \left(\frac{M_2}{M_1}\right)^{1{,}5} \quad (10)$$

Where:

$$K_e = 0{,}079 \times \frac{(M_1+M_2)^{\frac{3}{2}}}{M_1{}^{\frac{3}{2}} \times M_2{}^{\frac{1}{2}}} \times \frac{Z_1{}^{\frac{2}{3}} \times Z_2{}^{\frac{1}{2}}}{(Z_1{}^{\frac{2}{3}} + Z_2{}^{\frac{2}{3}})^{3/4}} \quad (11)$$

The nuclear stopping power of the target is defined as:

$$S_n(E) = 84{,}78 \times \frac{z_1 \times z_2}{\left(z_1^{\frac{2}{3}} + z_2 z^{\frac{2}{3}}\right)^{\frac{1}{2}}} \times \frac{M_1}{M_1 + M_2} \times S_n^{TF}(\varepsilon) \quad (12)$$

And we have:

$$S_n^{TF}(\varepsilon) = \frac{3{,}441 \times \sqrt{\varepsilon} \times \ln(\varepsilon - 1{,}708)}{1 + 6{,}355 \times \sqrt{\varepsilon} + \varepsilon(6{,}882 \times \sqrt{\varepsilon} - 1{,}708)} \quad (13)$$

Where:

$$\varepsilon = \frac{0{,}03255}{Z_1 \times Z_2 \left(Z_1{}^{2/3} + Z_2{}^{2/3}\right)^{1/2}} \times \frac{M_2}{M_1 + M_2} \times E(\text{ev}) \quad (14)$$

4 Evaluating Modeling Methods Against SRIM Calculations

This section aims to assess the accuracy of the SRIM program by comparing its results with analytical calculations based on the Yamamura-Tawara model. Our investigation specifically focused on the sputtering behavior of copper (Cu) materials, delving into how varying ion energy levels influence the sputtering yield. Through this analysis, we uncovered important insights regarding the relationship between energy levels and sputtering performance. This comparison not only enhances our understanding of the sputtering process but also reinforces the reliability of SRIM as a predictive tool in materials science.

Table 1. Simulation and theoretical results of sputtering yield analysis

E(Kev)	Theoretical results	Experimental results
0,1	0,645	0,652
1	3,77	3,71
10	8,84	8,13
100	5,76	5,94
1000	2,04	3,55
10000	0104	0,369

By juxtaposing the results obtained from SRIM with those derived from the Yamamura and Tawara models, we can evaluate the consistency and accuracy of SRIM in simulating ion energy loss. This comparative analysis not only validates the fundamental physical principles and assumptions underlying SRIM but also assesses the effectiveness of the Yamamura and Tawara models in capturing ion-matter interactions.

The correlation between the results from SRIM and those from the Yamamura and Tawara models, as illustrated in Table III.2, bolsters confidence in the reliability and precision of SRIM simulations. This enhanced understanding is crucial for predicting ion energy loss and sputtering yield phenomena effectively

5 Evaluating Ideal Parameters for Sputtering Yield Through SRIM Simulation.

The main goal of this study is to calculate the sputtering yield, represented as Y(E), using the Monte Carlo simulation program SRIM, which utilizes the binomial collision approximation (BCA) for ion-solid interactions. SRIM is an open-source software widely adopted for various practical applications. We investigated several angles of incidence (θ = [0°, 15°, 30°, 45°, 60°, 75°, 85°]) and different energy levels (E = [100 eV, 1 keV, 10 keV, 100 keV, 1000 keV]). The target materials—silicon (Si), copper (Cu), and indium oxide (In_2O_3)—were subjected to bombardment by gas ions (argon and xenon) in a vacuum chamber.

To achieve optimal results for any given material, it is essential to consider both the angle of incidence and the impact energy. Therefore, our primary focus is on identifying the collision energy (Emax) and angle of incidence (θmax) that result in the highest sputtering yield. These parameters indicate the maximum number of atoms ejected from the target material.

© 2025 NSP
Natural Sciences Publishing Cor.

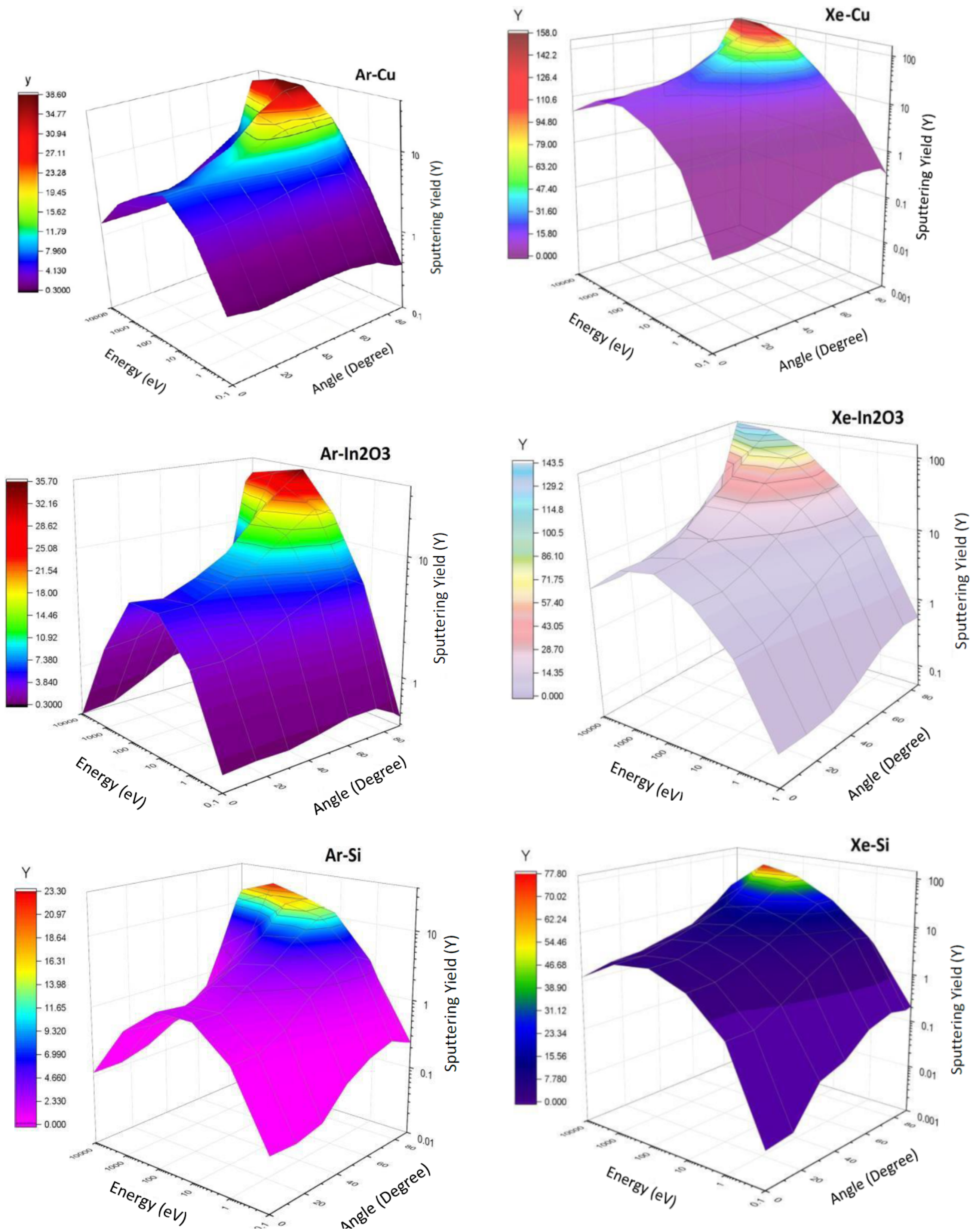

Figure 1. Sputtering Yield of Cu, Si, and In2O3 Materials Bombarded by Argon Gas at Various Energies and Incidence Angles

Figure 2. Sputtering Yield of Cu, Si, and In2O3 Materials Bombarded by Xenon Gas at Various Energies and Incidence Angles

Figures 1 and 2 present the sputtering yield rates for materials such as silicon (Si), indium oxide (In_2O_3), and copper (Cu) subjected to bombardment by argon (Ar) and xenon (Xe) plasma gas in a vacuum chamber. The experiments involved a range of energy levels and angles of incidence. The data indicate that the sputtering yield initially increases until it reaches a peak energy level, after which it begins to decline. This trend can be understood by analyzing the interaction between the ion beam and the target surface. At the peak energy levels, the ions have enough energy to displace atoms or molecules from the surface, thus enhancing the sputtering yield. However, when the energy exceeds this peak, the sputtering yield decreases due to a heightened risk of material damage caused by the excess ion energy.

The results also demonstrate different behaviors between argon and xenon gases, with xenon ions resulting in a greater sputtering yield compared to argon ions, attributed to xenon's larger atomic mass. A review of the figures reveals that sputtering yields vary based on the materials involved. Notably, silicon displays a relatively low sputtering yield, suggesting a lower tendency for atoms to be ejected from the surface during ion beam interaction. This characteristic can be linked to silicon's semiconductor properties and its ordered crystalline structure, which make it inherently more resistant to ejection when bombarded by ions.

In contrast, copper exhibits a higher sputtering yield compared to silicon due to its less ordered crystalline structure and the greater mobility of its atoms. This structural feature allows copper to be more easily ejected from the target surface, making it a preferred material for sputtering processes aimed at creating electrical conductors.

Indium oxide, however, shows a relatively high sputtering yield as well, which facilitates effective and uniform thin film deposition during the sputtering process. This tendency can be attributed to its chemical composition and crystalline structure, which enhance electrical conduction owing to its low resistivity during sputtering.

Table 2. Sputtering yield for bombardment ions (Ar and Xe) with an energy of 1.5 keV, varying across different incidence angles for Si, In2O3, and Cu materials

		0°	15°	30°	45°	60°	75°	85°	89°
Ar	Cu	4.70	4.92	5.57	6.59	7.84	7.35	5.21	3.51
	Si	0.703	0.704	1.21	2.11	3.87	5.39	4.42	2.79
	In203	3.25	3.35	3.62	4.87	6.81	7.86	6.43	4.07
Xe	Cu	2,72	2,73	3,90	6,26	8,86	9,24	6,85	4,65
	Si	0,521	0,582	1,16	2,36	4,74	7,54	6,44	3,99
	In203	2.32	2.313	3.02	5.20	8.34	10,60	8,76	5,78

Typical operating voltages in commercial and industrial sputtering applications range from 100 eV to 1.5 keV. Therefore, an optimal operating voltage of E_opt = 1.5 keV was chosen as the ideal energy source. Furthermore, the optimal incidence angle for maximizing sputtering yield for both gases was determined to be θ_opt = 75 degrees

6 Conclusion

The sputtering deposition process, essential for thin film production, is influenced by a variety of factors, including the choice of target material, the type of sputtering gas used, the angle of incidence, and the energy of the ion beam. These variables intricately affect the composition, structure, adhesion strength, and surface morphology of the resulting thin films. By carefully optimizing these parameters, manufacturers can create high-quality films with specific properties tailored for a wide range of applications.

For example, the selection of target material not only determines the chemical composition but also influences the crystalline structure and mechanical properties of the deposited film. Similarly, changing the sputtering gas can introduce certain chemical functionalities or modify the growth kinetics during deposition, which in turn affects the film's overall chemical and physical characteristics.

Additionally, the angle of incidence and the energy of the ion beam are critical in shaping the microstructure and morphology of the deposited film. Modifying the angle of incidence can alter the texture of the film, while the energy of the ion beam impacts the density of defects and the crystalline orientation within the film.

A thorough understanding of these complex interactions is vital for optimizing thin film fabrication processes to meet the rigorous demands of various applications. In electronics, where precise control over film thickness and electrical conductivity is crucial; in optics, where optical transparency and refractive index are essential; and in functional coatings, where durability and corrosion resistance are key, comprehending these variables ensures the development of thin films that excel in both performance and reliability.

References

[1] M. Koulali, A. Bouazza, "Enhancing the Sputtering Process with Plasma-Assisted Electrical Discharge for Thin Film Fabrication in Advanced Applications", *International Journal of Thin Film Science and Technology*, vol.13, no. 1, pp. 13-16. (2024), https://doi.org/10.18576/ijtfst/130102.

[2] A. Bouazza, " An Investigation by Monte Carlo Simulation of the Sputtering Process in Plasma". *J. Surf. Investig*. vol. 17, no. 5, 1172–1179 (2023). https://doi.org/10.1134/S1027451023050361.

© 2025 NSP
Natural Sciences Publishing Cor.

[3] A. Bouazza, “Revealing the role of vacuum chamber parameters on the pathways leading to substrate deposition by ejected atoms”, *International Journal of Thin Film Science and Technology*, vol. 12, no. 3,pp.159-162. (2023), https://doi.org/10.18576/ijtfst/120301.

[4] A. Bouazza, “3D Visualization of the Effect of Plasma Temperature on Thin-Film Morphology”, *Bull. Lebedev Phys. Inst*. 50, 7–13 (2023). https://doi.org/10.3103/S1068335623010037.

[5] A. Bouazza, “Investigation using Monte-Carlo codes simulations for the impact of temperatures and highpressures on thin films quality”, *Rev. Mex. Fís.,* vol. 69, no. 2 Mar-Apr, pp. 021501 1–, 2023, https://doi.org/10.31349/RevMexFis.69.021501.

[6] A. Bouazza, "Simulation of the Deposition of Thin-Film Materials Used in the Manufacturing of Devices with Miniaturized Circuits". *J. Surf. Investig*. vol. 16, no. 6, 1221–1230, 2022. https://doi.org/10.1134/S1027451022060283

[7] A. Bouazza, “Deposition of Thin Films Materials used in Modern Photovoltaic Cells”, *International Journal of Thin Film Science and Technology*, vol. 11, no. 3, pp. 313-320, 2022, https://doi.org/10.18576/ijtfst/110308

[8] A. Bouazza, “Sputtering of semiconductors, conductors, and dielectrics for the realization of electronics components thin-films”, *International Journal of Thin Film Science and Technology*, vol. 11, no. 2, pp. 225-232.2022, https://doi.org/10.18576/ijtfst/110210.

[9] S. E. C. Refas, A. Bouazza, and Y. Belhadji, “3D sputtering simulations of the CZTS, Si and CIGS thin films using Monte-Carlo method,” *Monte Carlo Methods Appl.*, vol. 27, no. 4, pp. 373–382, 2021, https://doi.org/10.1515/mcma-2021-2094.

10] A. Bouazza and A. Settaouti, “Understanding the contribution of energy and angular distribution in the morphology of thin films using Monte Carlo simulation,” *Monte Carlo Methods Appl*, 2018, https://doi.org/10.1515/mcma-2018-0019.

[11] A. Bouazza and A. Settaouti, “Monte Carlo simulation of the influence of pressure and target-substrate distance on the sputtering process for metal and semiconductor layers,” *Mod. Phys. Lett. B,* vol. 30, no. 20, pp. 1–18, 2016, https://doi.org/10.1142/S0217984916502535

[12] A. Bouazza and A. Settaouti, “Study and simulation of the sputtering process of material layers in plasma,” *Monte Carlo Methods Appl*., vol. 22, no. 2, pp. 149–159, 2016, https://doi.org/10.1515/mcma-2016-0106.

[13] Hassan, M. A., et al. “Monte Carlo Simulation Model for Magnetron Sputtering Deposition.” Advanced Materials Research, vol. 1105, *Trans Tech Publications, Ltd.,* May 2015, pp. 69–73. https://doi.org/10.4028/www.scientific.net/amr.1105.69.

[14] DEPLA, Diederik et LEROY, W. P. Magnetron sputter deposition as visualized by Monte Carlomodeling. Thin Solid Films, 2012, vol. 520, no 20, p. 6337-6354. https://doi.org/10.1016/j.tsf.2012.06.032.

[15] MALAURIE, A. et BESSAUDOU, A. Numerical simulation of the characteristics of the different metallic species falling on the growing film in dc magnetron sputtering. *Thin Solid Films*, 1996, vol. 286, no1-2, p. 305-316. https://doi.org/10.1016/S0040-6090(95)08523-8

[16] Kersch, A., W. Morokoff, and Chr Werner. "Self-consistent simulation of sputter deposition with the Monte Carlo method." *Journal of applied physics* 75.4 (1994): 2278-2285. https://doi.org/10.1063/1.356292

[17] A. Bouazza, "Characterizing the Relationship Between Sputtered Atom Flux Generated by Electrical Discharge in Plasma and Thin Film Deposition Quality". *International Journal of Thin Film Science and Technology*, vol. 13, no. 2, pp. 95-100. (2024), https://doi.org/10.18576/ijtfst/130202

[18] GERGS, Tobias, MUSSENBROCK, Thomas, et TRIESCHMANN, Jan. A Molecular Dynamics Studyon the Role of Ar Ions in the Sputter Deposition of Al Thin Films. arXiv preprint arXiv:2110.00356, 2021. https://doi.org/10.48550/arXiv.2110.00356.

[19] COON, S. R., CALAWAY, W. F., BURNETT, J. W., et al. Yields and kinetic energy distributions of sputtered neutral copper clusters. Surface science, 1991, vol. 259, no 3, p. 275-287. https://doi.org/10.1016/0039-6028(91)90558-A

[20] A. Bouazza, "Optimization of the Cathodic Sputtering Process for Fabricating Thin Film Materials used in Modern Photovoltaic Applications". *International Journal of Thin Film Science and Technology*, vol. 13, no. 2, pp. 101-115. (2024), https://doi.org/10.18576/ijtfst/130203.

© 2025 NSP
Natural Sciences Publishing Cor.